

The *Saccharomyces cerevisiae* *MLH3* gene functions in MSH3-dependent suppression of frameshift mutations

HERNAN FLORES-ROZAS AND RICHARD D. KOLODNER[†]

Ludwig Institute for Cancer Research, Cancer Center and Department of Medicine, University of California, San Diego School of Medicine, La Jolla, CA 92093

Edited by Nicholas R. Cozzarelli, University of California, Berkeley, CA, and approved August 13, 1998 (received for review June 23, 1998)

ABSTRACT The *Saccharomyces cerevisiae* genome encodes four MutL homologs. Of these, MLH1 and PMS1 are known to act in the MSH2-dependent pathway that repairs DNA mismatches. We have investigated the role of MLH3 in mismatch repair. Mutations in *MLH3* increased the rate of reversion of the *hom3-10* allele by increasing the rate of deletion of a single T in a run of 7 Ts. Combination of mutations in *MLH3* and *MSH6* caused a synergistic increase in the *hom3-10* reversion rate, whereas the *hom3-10* reversion rate in an *mlh3 msh3* double mutant was the same as in the respective single mutants. Similar results were observed when the accumulation of mutations at frameshift hot spots in the *LYS2* gene was analyzed, although mutation of *MLH3* did not cause the same extent of affect at every *LYS2* frameshift hot spot. MLH3 interacted with MLH1 in a two-hybrid system. These data are consistent with the idea that a proportion of the repair of specific insertion/deletion mispairs by the MSH3-dependent mismatch repair pathway uses a heterodimeric MLH1-MLH3 complex in place of the MLH1-PMS1 complex.

Mismatch repair safeguards the integrity of the genome by recognizing and correcting mispaired bases that arise because of misincorporation of nucleotides during DNA replication (reviewed in refs. 1 and 2) or as a result of chemical damage to DNA and DNA precursors (3–5). Mismatch repair recognizes mispaired bases present in heteroduplex recombination intermediates and it can prevent recombination between divergent DNAs (6–8). The crucial role of mismatch repair proteins in the stabilization of the genome is illustrated by the finding that inactivation of certain human mismatch repair genes that are related to the bacterial *mutS* and *mutL* genes underlie both inherited cancer susceptibility syndromes (reviewed in ref. 9) and sporadic cancers (10–12).

The best understood mismatch repair pathway involving MutS and MutL-type proteins is the *Escherichia coli* MutHLS mismatch repair pathway (reviewed in refs. 1 and 2). This reaction has been reconstituted *in vitro* by using hemimethylated DNA substrates containing mismatches, MutH, MutL, MutS, and UvrD (helicase II) proteins along with DNA polymerase III holoenzyme, DNA ligase, single-stranded DNA binding protein, and any one of the single-stranded DNA exonucleases-exo I, exo VII, or RecJ protein, or possibly other exonucleases (13). This basic mismatch repair system is present in eukaryotes, although less is known about the relevant eukaryotic proteins or how they function in mismatch repair.

In yeast, humans, and mice, several genes that encode homologs of MutS and MutL have been cloned. *Saccharomyces cerevisiae* has six genes encoding proteins related to MutS, *MSH1-6*, three of which function in mismatch repair in the nucleus (1, 14). Repair is carried out by two different MSH2-dependent pathways (15). One involves a complex of MSH2

and MSH6 that repairs base-base mispairs and small insertion/deletion mispairs. The second requires a complex of MSH2 and MSH3 and corrects insertion/deletion mispairs. Similarly, human MSH2 appears to function as a complex with either MSH6 or MSH3 (16–18). Homologs of MutL also are found in eukaryotes. In yeast, two MutL homologs, MLH1 and PMS1, exist as a heterodimer and this complex appears to function in an analogous manner to *E. coli* MutL (19, 20). In humans, two MutL homologs, MLH1 and PMS2 (the human homolog of yeast PMS1) also function in mismatch repair as a heterodimeric complex (21). A third human MutL homolog, PMS1, has been suggested to function in mismatch repair by the finding of a germ-line mutation in this gene in a patient with a history of colon cancer (22) but a biochemical role for this protein in mismatch repair has not been demonstrated.

Recently, two additional MutL homologs have been revealed by the *S. cerevisiae* genome sequence project, *MLH2* (ORF YLR035c) and *MLH3* (ORF YPL164c) (14). In addition, a fragment of MLH3 was identified in a two-hybrid screen using MLH1 as bait because the C-terminal region of MLH3 appears to contain a MLH1 interaction sequence (23). The role of these two MutL homologs in mismatch repair has not yet been elucidated; however, the ability of a fragment of MLH3 to interact with MLH1 suggests a role for MLH3 in some type of MLH1-dependent reaction.

MATERIALS AND METHODS

General Genetic Methods. Yeast extract/peptone/dextrose media, sporulation media, synthetic drop-out media, 5-fluoroorotic acid, and canavanine-containing media were as described (24, 25).

Strains. All strains used in this study are isogenic derivatives of RDKY3023, a strain derived from S288c (Table 1). Strains were constructed by gene disruption as described (26, 27) and verified by PCR. RDKY2402-*mlh3* strain was constructed by replacing nucleotides +26 to +2,094 of the 2,119-nt *MLH3* ORF with the *HIS3* gene by using PCR-mediated gene disruption. The required PCR product was generated by amplification of the *HIS3* gene present in pRS423 (28) with primers HFR021 5'-GTGAAGCTC-GTCAACTCAAAAAGAAAATGAGCCAGCATATTAGG-AAATTAGAgagcagattgtactgagagtgacc and HFR022 5'-GTTCCAGGATTAAGGTTCTCTTTACTTCAATTCTGCAAT-GGGTACCATAGctccttaccgatctgtgctggtatttc (uppercase characters correspond to *MLH3*-specific sequence and the lowercase sequences flank the selective marker present in plasmid containing the *HIS3* gene).

RDKY2419-*msh6::hisG* was generated by using the *EcoRI/SphI* disruption fragment from plasmid pEAI108 that results in the replacement of nucleotides +108 to +3,000 of the 3,725-nt *MSH6* ORF with a *hisG-URA3-hisG* cassette. Excision of the *URA3* marker by recombination between the *hisG* repeats resulting in the *msh6::hisG* derivative was selected for on min-

The publication costs of this article were defrayed in part by page charge payment. This article must therefore be hereby marked "advertisement" in accordance with 18 U.S.C. §1734 solely to indicate this fact.

© 1998 by The National Academy of Sciences 0027-8424/98/9512404-6\$2.00/0
PNAS is available online at www.pnas.org.

This paper was submitted directly (Track II) to the *Proceedings* office.
[†]To whom reprint requests should be addressed: Ludwig Institute for Cancer Research, University of California, San Diego School of Medicine, CMME3080, 9500 Gilman Drive, La Jolla, CA 92093-0660.
e-mail: rkolodner@ucsd.edu.

Table 1. *S. cerevisiae* strains used in this study

RDKY3023: wild type*
RDKY2402: <i>mlh3::HIS3</i>
RDKY2419: <i>msh6::hisG</i>
RDKY2431: <i>msh3::hisG</i>
RDKY2407: <i>mlh1::hisG-URA3-hisG</i>
RDKY2750: <i>pms1::hisG</i>
RDKY2405: <i>mlh3::HIS3, msh6::TRP1</i>
RDKY2408: <i>mlh1::hisG-URA3-hisG, mlh3::HIS3</i>
RDKY2412: <i>mlh3::TRP1, pms1::hisG</i>
RDKY2403: <i>mlh3::HIS3, msh3::TRP1</i>
RDKY2404: <i>mlh3::HIS3, msh2::hisG</i>
RDKY2707: <i>msh2::hisG</i>
RDKY3535: <i>msh3::TRP1, msh6::hisG</i>

*All strains containing the following markers: *MAT a, ura3-52, leu2Δ1, trp1Δ63, his3Δ200, lys2ΔBgl, hom3-10, ade2Δ1, ade8*.

imal drop-out plates containing 5-fluoroorotic acid. RDKY2431-*msh3::hisG* was similarly constructed by using an *EcoRI* fragment containing a *hisG-URA3-hisG* cassette replacing nucleotides +638 to +3,135 of the 3141-nt *MSH3* ORF derived from plasmid pEN33. RDKY2750-*pms1::hisG* was constructed by replacing nucleotides +168 to +2,231 of the 2,712-nt *PMS1* ORF with the *hisG-URA3-hisG* containing *SalI* fragment of plasmid pEAI100. The *MLH1* gene was disrupted with *hisG* in the isogenic strain RDKY2669 (α , *ura3-52, leu2Δ1, trp1Δ63, his3Δ200, lys2ΔBgl, hom3-10, ade2Δ1, ade8*) using the *hisG-URA3-hisG* cassette present in the *SphI/KpnI* fragment of plasmid pEAI105, which removes nucleotides +34 to +2,303 of the 2,305-nt *MLH1* ORF generating strain RDKY2407-*mlh1::hisG*.

Strain RDKY2408-*mlh3 mlh1* was generated by crossing strains RDKY2402-*mlh3* and RDKY2407-*mlh1* followed by tetrad dissection and genotyping. The strain RDKY2412-*mlh3 pms1* was generated by disrupting the *MLH3* gene in strain RDKY2750-*pms1* as described for RDKY2402, except that the *TRP1* gene present in plasmid pRS424 was amplified by using oligonucleotides HFR021 and HFR022 and used as the disruption marker. Strain RDKY2403-*mlh3 msh3* was generated by replacing nucleotides +45 to +3,160 of the 3,140-nt *MSH3* ORF in RDKY2402-*mlh3* using a PCR fragment obtained by amplifying the *TRP1* gene of pRS424 using oligonucleotides HFR307 5'-GAACAATGGTGATAGGTAATGAACCTA-AACTGGTACTTTTGAGAGCCAAAAGagcagattgtactgagagtgcacc and HFR308 5'-GCTGCATTTAGAACATACGTACCATCCGCATCAGTGGATATCCAATGATAGctcttaccgatctgtgcggtatttc. Strain RDKY2405-*mlh3 msh6* was generated by transforming strain RDKY2402-*mlh3* with a PCR product containing the *TRP1* gene amplified from plasmid pRS424 with oligonucleotides HFR011 5'-CTCCAAAA-TGGCCCCAGCTACCCCTAAAACCTTCTAAGACTGCA-CACTTCGAAAgagcagattgtactgagagtgcacc and HFR012 5'-CGTAAATGAAAATACTTAGGATTGTAAATCATCAATTATACTAAATAGACTctcttaccgatctgtgcggtatttc which replaces nucleotides +34 to +3,692 of the 3,725-nt *MSH6* ORF with *TRP1*. The *MSH2* ORF was disrupted in strain RDKY2402-*mlh3* by transforming with a *PvuII/AatII* restriction fragment of plasmid pEAI98 that carries the *msh2::hisG-URA3-hisG* cassette. The resulting strain, RDKY2404-*mlh3 msh2*, has nucleotides +1 to +2,694 of the 2,895-nt *MSH2* ORF replaced by *hisG* sequences. Strain RDKY3535-*msh6::hisG msh3::TRP1* was generated by replacing the *MSH3* ORF in RDKY2419-*msh6* as described above for strain RDKY2403. Strain RDKY2707-*msh2::hisG* has been previously described (25).

Mutation Analysis. Mutation rates were determined by fluctuation analysis using at least five independent colonies (15, 25, 29). Each fluctuation test was repeated at least twice. Spectrum analysis was carried out by selecting revertants (Lys^+

or Thr^+) or mutants (Can^r) on selective minimum media drop-out plates. Chromosomal DNA was isolated from the revertants (30) and the relevant regions of *LYS2, HOM3*, and *CAN1* were amplified by PCR and sequenced (15, 25).

DNA Sequence Analysis. All DNA sequencing was performed by using an Applied Biosystems 377 DNA sequencer and standard chemistry. Analysis of the sequence chromatograms was carried out by using Sequencher (Gene Codes, Ann Arbor, MI), and sequence comparisons, alignments, and phylogenetic trees were generated by using DNASTar software (Madison, WI). Database searches were performed by using the BLAST algorithm (<http://genome-www2.stanford.edu/cgi-bin/SGD/nph-blast2sgd>). The determination of sequence identity between two homologs was performed by using the FASTA algorithm available at <http://genome.eerie.fr/bin/align-guess.cgi>.

Plasmids. The yeast *MLH3* gene was amplified from genomic DNA by PCR using oligonucleotides HFR300 5'-CGGTTAGCACGAATTCACCATGAGCCAGCATATTAG-GAAATTAG and HFR302 5'-GGTCGACGCGTAAGCTT-TACTTCAATTCGCAATGGGTACCATAG, and cloned into pYX243 (Novagen) to yield pRDK742. The entire *MLH3* ORF was excised from pRDK742 as an *EcoRI/XhoI* fragment and cloned into pEG202 (31) to generate *MLH3*-bait plasmid pRDK743. The *MLH1* prey construct, pRDK744, was generated by cloning a PCR fragment obtained by amplifying *MLH1* from pEN71 (20, 32) using oligonucleotides HFR601 5'-ATCGAATTCGGCCTAGGGATGTCTCTCAGAATAAAA-GCACTT and HFR602 5'-TCTCACGCTCGCTCGAGTTA-ACACCTCTCAAAAACCTTTGTAT into the *AvrII* and *XhoI* sites of pJG4-5* [pJG4-5 (31) modified in this laboratory by Pascale Bertrand]. The *PMS1* prey plasmid (pRDK745) was constructed by amplifying *PMS1* from pRDK433 (constructed in this laboratory by Ruchira Das Gupta) using oligonucleotides HFR603 5'-ATCGAATTCGGCCTAGGGATGTTTACCACATCGAAAACCTTA and HFR602, and inserting the resulting fragment between the *AvrII* and *XhoI* sites of pJG4-5*. The presence of the relevant wild-type sequence in all plasmids was confirmed by DNA sequencing.

Interaction Experiments. Yeast strain RDKY2926 [strain EGY48 harboring reporter plasmid pSH18-34 (33, 34)] was simultaneously transformed with a LexA-fusion bait construct (either pEG202 or pRDK743-*MLH3*) and an acid activation-tagged prey construct (pJG4-5*, pRDK745-*PMS1*, or pRDK744-*MLH1*) and selected on $\text{Ura}^- \text{His}^- \text{Trp}^-$ minimal drop-out plates. Isolates were tested for interaction by replica plating onto minimal media drop-out plates containing galactose and 5-bromo-4-chloro-3-indolyl β -D-galactoside (31, 35).

RESULTS

Identification of *MLH3*. In addition to *MLH1* and *PMS1*, two ORFs with homology to bacterial MutL can be identified in the *S. cerevisiae* Genome Database using BLAST searches, ORF YLR035c, which has been previously termed *MLH2* (1, 14), and ORF YPL164c called *MLH3* (14, 23). The molecular weight of the predicted *MLH3* protein is 81,997. In comparison to different MutL homologs, *MLH3* appears to be most closely related to human *PMS1* (Fig. 1). The observed sequence identity (20%) and similarity (47%) between yeast *MLH3* and human *PMS1* is comparable to that observed for other yeast and human *MSH* and *MLH* proteins known to be functional homologs.

Strains Deficient in *MLH3* Display a Mutator Phenotype. To investigate a possible role of *MLH3* in mismatch repair, we constructed a series of isogenic mutant strains deleted for *MLH3* and other mismatch repair genes (Table 1). The *mlh3* mutant strain was viable, had no growth phenotype, exhibited the same sensitivity to alkylating agents (methyl methane sulfonate) and UV irradiation as the wild type, and was able to grow in media containing nonfermentable sugars (data not shown). The *mlh3* mutant strain also was examined for mutator phenotypes by

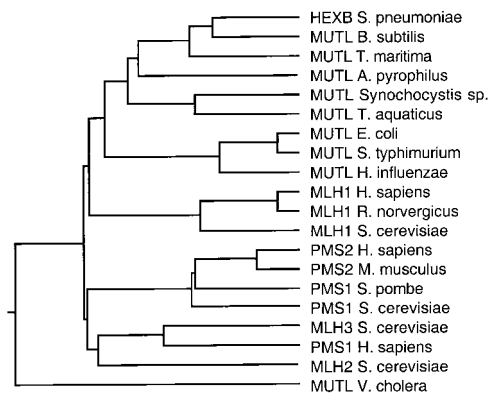


FIG. 1. Phylogenetic tree of MutL-related proteins. The dendrogram was generated with Megalign (DNASStar) by the clustal method with the weight table set to identities, a gap penalty of 10, and a gap length penalty of 10. All sequences used are full length and were retrieved from GenBank.

determining the rate of reversion of the *hom3-10* and *lys2-Bgl* alleles and the rate of accumulation of Can^r mutations.

Compared with the wild type, an increase in the rate of reversion of *hom3-10* and *lys2-Bgl*, two assays that are particularly sensitive to defects in mismatch repair, was observed in the *mlh3* strain (3.3- and 2.2-fold, respectively). There was no significant increase in the rate of accumulation of Can^r mutants (Table 2). This phenotype closely resembles that exhibited by *msh3* strains (Table 2) (15, 36), suggesting that *MLH3* and *MSH3* could function in the same pathway. Consistent with this finding, the *mlh3 msh3* double mutant had essentially the same rate of reversion of *lys2-Bgl* and *hom3-10* and the same rate of accumulation of Can^r mutations as either single mutant strain (Table 2). A *msh6* mutant showed a substantial increase in the rate of accumulation of Can^r mutations but only had a modest increase in the reversion rate of *hom3-10* and *lys2-Bgl*. This finding agrees with previous results indicating that *msh6* mutants are defective in repair of base-base mispairs but only show small defects in the repair of insertion/deletion mispairs (15, 37). The reversion rate for the *hom3-10* allele was greatly increased in a *msh6 mlh3* double mutant compared with either single mutant (Table 2). Reversion of the *lys2-Bgl*

Table 2. Mutation rate analysis of *mlh3* and other mismatch repair-deficient strains

Strain	Mutation rate		
	Thr ⁺	Lys ⁺	Can ^r
Wild type	1.2 × 10 ⁻⁸ (1.0)	1.0 × 10 ⁻⁸ (1.0)	2.4 × 10 ⁻⁷ (1.0)
<i>mlh3</i>	3.9 × 10 ⁻⁸ (3.3)	2.2 × 10 ⁻⁸ (2.2)	2.8 × 10 ⁻⁷ (1.2)
<i>msh3</i>	5.5 × 10 ⁻⁸ (4.6)	2.1 × 10 ⁻⁸ (2.1)	3.1 × 10 ⁻⁷ (1.3)
<i>mlh3 msh3</i>	5.9 × 10 ⁻⁸ (4.9)	2.9 × 10 ⁻⁸ (2.9)	4.0 × 10 ⁻⁷ (1.6)
<i>msh6</i>	9.1 × 10 ⁻⁸ (7.6)	2.3 × 10 ⁻⁸ (2.3)	2.9 × 10 ⁻⁶ (12)
<i>mlh3 msh6</i>	8.2 × 10 ⁻⁷ (68)	4.6 × 10 ⁻⁸ (4.6)	3.1 × 10 ⁻⁶ (13)
<i>msh2</i>	6.7 × 10 ⁻⁶ (558)	4.8 × 10 ⁻⁷ (48)	2.9 × 10 ⁻⁶ (12)
<i>mlh3 msh2</i>	5.1 × 10 ⁻⁶ (425)	4.3 × 10 ⁻⁷ (43)	2.9 × 10 ⁻⁶ (12)
<i>msh3 msh6</i>	5.7 × 10 ⁻⁶ (475)	5.9 × 10 ⁻⁷ (59)	2.7 × 10 ⁻⁶ (11)
<i>mlh1</i>	5.5 × 10 ⁻⁶ (458)	4.8 × 10 ⁻⁷ (48)	3.9 × 10 ⁻⁶ (16)
<i>mlh3 mlh1</i>	6.6 × 10 ⁻⁶ (545)	7.9 × 10 ⁻⁷ (79)	3.9 × 10 ⁻⁶ (16)
<i>pms1</i>	3.6 × 10 ⁻⁶ (300)	5.1 × 10 ⁻⁷ (51)	3.1 × 10 ⁻⁶ (13)
<i>mlh3 pms1</i>	9.7 × 10 ⁻⁶ (804)	5.0 × 10 ⁻⁷ (50)	5.8 × 10 ⁻⁶ (21)

Mutation rates were calculated by using the method of the median using five independent colonies per experiment. The average of several experiments is presented. The number of tests carried out with each strain is as follows: wild type, five times; *mlh3*, six times; *msh6*, *mlh3 msh6*, and *msh3 msh6*, three times each; *msh3*, *mlh3 msh3*, *msh2*, and *mlh3 msh2*, twice each. For *mlh1*, *mlh3 mlh1*, *pms1*, and *mlh3 pms1*, the test was repeated twice. The fold increase in the mutation rate compared to the wild-type strain is shown in parentheses.

allele was increased to a lesser, but significant, extent in the *msh6 mlh3* double mutant compared with each single mutant. In contrast, the rate of accumulation of Can^r mutations was the same in the *msh6 mlh3* strain compared with the *msh6* single mutant. This genetic interaction between *mlh3* and *msh6* mutations is consistent with the idea that *MLH3* participates in the repair of some insertion/deletion mispairs by the *MSH3* pathway.

Analysis of the Spectrum of Mutations in *mlh3* Mutants. To further characterize the possible role of *MLH3* in mismatch repair, we analyzed the spectrum of mutations causing the increased reversion of the *hom3-10* and *lys2-Bgl* alleles seen in *mlh3* mutants. As previously described, the *hom3-10* allele carries an additional T in a run of six Ts, resulting in a +1 frameshift (15). As shown in Fig. 2, reversion occurs predominantly by deletion of the extra T in the mononucleotide run. In the wild-type strain, 21% (5/24) of the reversions occurred at sites different from the T tract. In the *mlh3* and *msh6* single mutants, the number of mutations at sites other than the run of Ts was 4% (1/24) and 14% (4/28), respectively, whereas in the *msh6 mlh3* double mutant, reversion occurred exclusively at the T tract (30/30).

When the mutation rates presented in Table 2 are recalculated by using the mutation spectra data to obtain rates for mutation at a specific site (Table 3) (38), we find that reversions arising exclusively at the T tract in *hom3-10* occur at a rate of 9.5×10^{-9} in the wild-type strain. For *mlh3*, the rate is 3.9-fold higher than that of wild-type cells. The rate for *msh6* is 8.6-fold higher than wild type, whereas the reversion rate at this site in the *mlh3 msh6* double mutant is 86-fold higher than that of wild-type cells. This latter 86-fold increase is about 15% of the events seen at this site in a *msh2* mutant strain. These results suggest that *mlh3* mutations cause a defect in repair of insertion/deletion mispairs that result because of replication errors at mononucleotide runs and that this defect is most pronounced when *MSH6*-dependent mismatch repair has been inactivated.

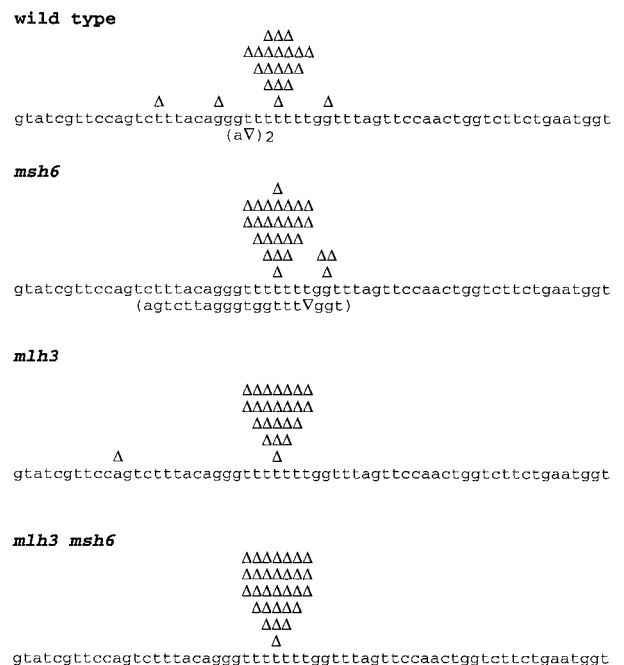


FIG. 2. Spectra of mutations reverting the *hom3-10* allele in wild-type and different mutant strains. Nucleotides 623–682 of the sequenced region is shown. Each independent frameshift event detected is indicated over the sequence with a Δ . Complex mutations that include base changes are shown below the sequence in parentheses. In the wild-type strain, two identical complex events were observed. The total number of isolates analyzed was: wild type, 24; *msh6*, 28; *mlh3*, 24, and *mlh3 msh6*, 30.

Table 3. Mutation rates at the *hom3-10* and *lys2-Bgl* hotspots

Strain	Mutation rate			
	<i>hom3-10</i>		<i>lys2-Bgl</i>	
	T ₆₄₆₋₆₅₂	A ₃₆₄₋₃₆₉	C ₄₀₁₋₄₀₄	T ₄₁₇₋₄₁₉
Wild type	9.5 × 10 ⁻⁹ (1.0)	0.2 × 10 ⁻⁸ (1.0)	0.13 × 10 ⁻⁸ (1.0)	0.05 × 10 ⁻⁸ (1.0)
<i>mlh3</i>	3.7 × 10 ⁻⁸ (3.9)	1.1 × 10 ⁻⁸ (5.5)	0.44 × 10 ⁻⁸ (3.4)	0.04 × 10 ⁻⁸ (0.9)
<i>msh3</i>	N.D.	1.1 × 10 ⁻⁸ (5.5)	0.18 × 10 ⁻⁸ (1.4)	<0.04 × 10 ⁻⁸ (<1)
<i>mlh3 msh3</i>	N.D.	1.4 × 10 ⁻⁸ (7.0)	0.5 × 10 ⁻⁸ (3.8)	0.15 × 10 ⁻⁸ (3.0)
<i>msh6</i>	9.1 × 10 ⁻⁸ (8.6)	0.23 × 10 ⁻⁸ (1.2)	0.23 × 10 ⁻⁸ (1.8)	0.76 × 10 ⁻⁶ (15.2)
<i>mlh3 msh6</i>	8.2 × 10 ⁻⁷ (86)	2.9 × 10 ⁻⁸ (14.5)	0.6 × 10 ⁻⁸ (4.6)	0.23 × 10 ⁻⁶ (4.6)

Mutation rates were recalculated based on the frequency of occurrence of frameshifts at the indicated sites. N.D., not determined (see Table 2 for gross mutation rates at this site).

The analysis of the spectra of the *lys2-Bgl* revertants indicates that reversion can occur by mutations within a window of approximately 150 bp (Fig. 3) (15, 25, 39). In contrast to the wild-type strain, the distribution of revertants in the mismatch repair-deficient strains appears to be nonrandom and three mutation hot spots account for most of the reversion events (Fig. 3). Mutations were found to occur at significantly higher rates at a run of six As (A₃₆₄₋₃₆₉), a run of four Cs (C₄₀₁₋₄₀₄), and a run of three Ts (T₄₁₇₋₄₁₉). Furthermore, there were significant differences between the mutation spectra observed in the different mutant strains analyzed. As shown in Fig. 3, the most notable mutation hot spot in the *msh6* strain was the T₄₁₇₋₄₁₉ site where 33% (14/42) of the mutations were found versus 5% (2/40) in the wild-type strain. The distribution of mutations at the other sites was 10% (4/42) at A₃₆₄₋₃₆₉ and 10% (4/42) at C₄₀₁₋₄₀₄ for the *msh6* mutant strain and 20% (8/40) at A₃₆₄₋₃₆₉ and 13% (5/40) at C₄₀₁₋₄₀₄ in the wild-type strain, respectively. The spectra of mutations seen in the *mlh3* and *msh3* mutants had similar patterns with 50% (23/46) and 52% (24/46) of the frameshifts occurring at the A₃₆₄₋₃₆₉ site in the *mlh3* and *msh3* mutant strains, respectively. The *mlh3 msh3* double mutant had the same spec-

trum of the frameshifts (49%, 20/41 at A₃₆₄₋₃₆₉) as observed in the respective single mutants. The proportion of frameshifts at the A₃₆₄₋₃₆₉ site observed in the *mlh3 msh6* double mutant (63%, 32/51) was quite different from that seen in the *msh6* single mutant.

When the mutation rates at individual sites were calculated (Table 3), we found that the rate of reversion at the A₃₆₄₋₃₆₉ site in the *mlh3* strain was 5.5-fold greater than that of wild type and similar to that of *msh3* (5.5-fold greater than wild type) and *mlh3 msh3* mutants (7-fold greater than wild type). The *msh6* strain did not show an increase in the mutation rate at this site compared with the wild type. In contrast, a 14.5-fold increase in the reversion rate at this site was observed for the *mlh3 msh6* strain. These data demonstrate (i) a synergistic effect on the rate of mutation at the A₃₆₄₋₃₆₉ site in the *mlh3 msh6* double mutant and (ii) that the *mlh3 msh3* double mutant shows a mutation rate at this site that is not significantly different to that seen for the respective single mutants. These observations are consistent with the results obtained with the *hom3-10* reversion assay and suggest that *MLH3* functions in the *MSH3* pathway and not in the *MSH6* pathway.

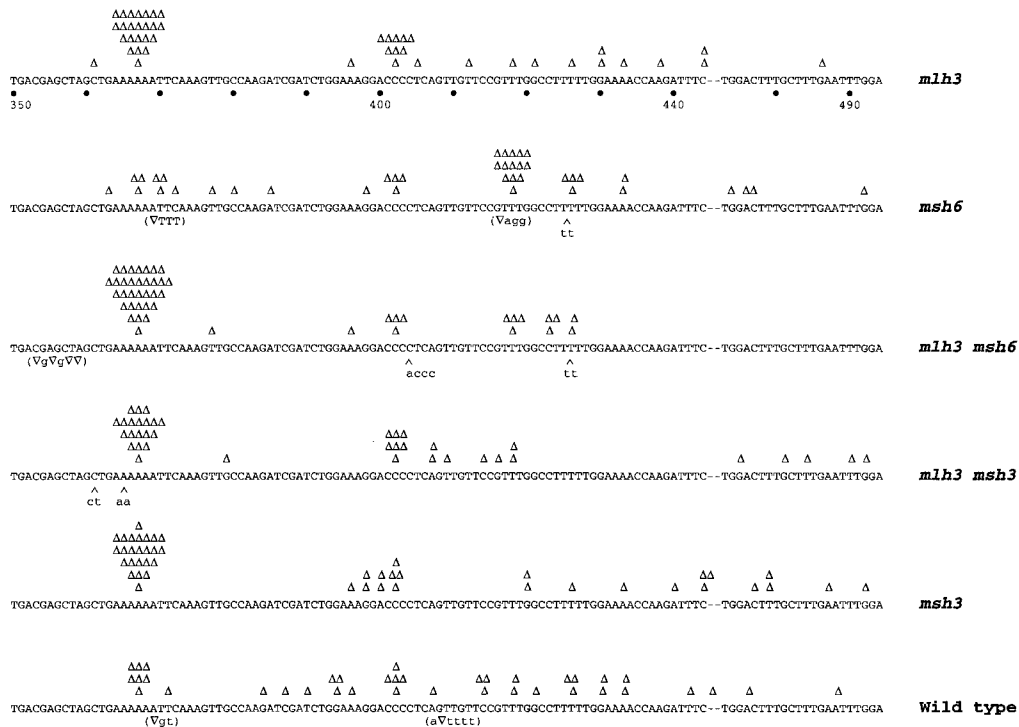


FIG. 3. Spectra of mutations reverting the *lys2-Bgl* allele in wild-type and different mutant strains. The region comprising nucleotides 350–444 and 473–494 is shown. Each frameshift reversion is indicated on top of the sequence depicted by a Δ. Reversion events involving single basepair deletions and base changes are shown in parentheses below the sequence and insertions are indicated by a ^. The deletion of an A occurring at position 467 in a revertant of the wild-type strain is indicated over the -. The number of revertants analyzed was: wild type, 40; *msh6*, 42; *mlh3*, 46; *mlh3 msh6*, 51; *msh3*, 46; *mlh3 msh3*, 41.

A similar analysis of the effect of *mlh3* mutations on mutation rates at the other *lys2-Bgl* reversion hot spots also was performed (Table 3). The mutation rate at the C_{401–404} site in the *mlh3* strain was 3.4-fold greater than wild type and was similar to that of *msh3* (1.4-fold greater than wild type) and *mlh3 msh3* strains (3.8-fold greater than wild type). For *msh6*, the mutation rate was 1.8-fold greater than wild type, whereas for the *mlh3 msh6* strain a 4.6-fold increase was observed. The mutation rate at the T_{417–419} site in *mlh3* mutants was the same as in the wild type and, similarly, no significant increase in the reversion rate at this site was found for *msh3* (<1-fold greater than wild type). However, in *msh6*, 33% of the reversion events occurred at the T_{417–419} site, resulting in a rate increase that was 15.2-fold greater than wild type. Modest increases were obtained for *mlh3 msh3* (3.0-fold greater than wild type) and *mlh3 msh6* strains (4.6-fold greater than wild type). These data suggest that there is little, if any, effect of mutations in *MLH3* on the accumulation of frameshift mutations at the C_{401–404} and T_{417–419} sites, and that the effect at these sites is not as large as at the *lys2-Bgl* A_{364–369} site or the *hom3–10* site.

Interaction Between MLH1 and MLH3. In eukaryotes, MutL homologs have been shown to function as heterodimers (19, 21, 23, and reviewed in refs. 1 and 2). To examine the possibility that MLH3 also may function as part of a heterodimer with another MutL homolog, a series of strains containing different combinations of mutations in genes encoding MutL homologs were constructed (Table 1). Strains containing deletion mutations in *MLH1* and *PMS1* displayed high mutation rates similar to those observed in *msh2* strains and *msh3 msh6* double mutant strains (Table 2). No significant difference was observed between strains carrying a deletion of *MLH1* and strains deleted for both *MLH1* and *MLH3*, consistent with *MLH1* being epistatic to *MLH3*. On the other hand, the rate of reversion of the *hom3–10* allele in the *pms1 mlh3* double mutant was significantly higher than that observed in the *pms1* single mutant ($P < 0.05$, Mann–Whitney U test) but not significantly higher than observed in the *msh2* single mutant ($P < 0.05$, Mann–Whitney U test, Table 2), suggesting that MLH3 and PMS1 may function in different repair pathways.

Pang *et al.* (23) identified a C-terminal fragment of MLH3 by virtue of its ability to interact with MLH1 in a two-hybrid screen and further demonstrated that MLH3 has significant homology to PMS1 in the C-terminal region required for interaction with MLH1. To extend these results and demonstrate that full-length MLH3 can interact with MLH1, the interaction between MLH3 and MLH1 was analyzed using a two-hybrid–based system. A bait construct expressing MLH3 fused to the LexA DNA-binding domain was cotransformed with plasmids carrying either PMS1 or MLH1 fused to an acid activation domain, or a control plasmid carrying only the activation domain, into a strain carrying the *LacZ* reporter gene in a plasmid, under the control of a GAL1 promoter (31, 35). Activation of the reporter gene was only observed only when MLH3 and MLH1 were coexpressed in the same cell, suggesting an interaction between MLH3 and MLH1 (Fig. 4). There was no activation of the reporter gene when the MLH1 or PMS1 prey plasmids were cotransformed with plasmids containing only the LexA DNA-binding domain, indicating that the observed interaction of MLH3 and MLH1 required the expression of both proteins.

DISCUSSION

A model (reviewed in ref. 1) has been proposed for the role of MutS and MutL homologs in eukaryotic mismatch repair (Fig. 5). Mismatch recognition involves two different heterodimeric complexes of MutS-related proteins, MSH2–MSH6 and MSH2–MSH3. These two complexes are partially redundant with regard to their mismatch recognition specificity. In *S. cerevisiae*, the MSH2–MSH6 complex functions in the repair of base-base and small insertion/deletion mismatches but probably plays only a limited role in the repair of larger insertion/deletion mismatches (larger than two unpaired bases) (15, 37). In contrast, the MSH2–MSH3 complex does not likely recognize base-base mismatches but rather

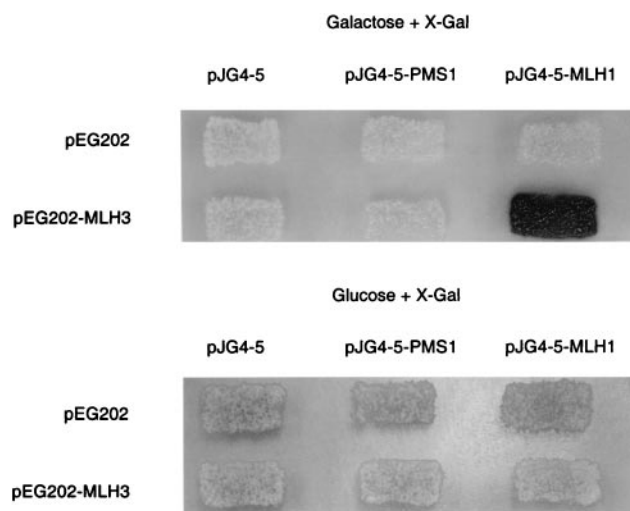


FIG. 4. Interaction of MLH3 and MLH1 by two-hybrid analysis. Yeast strain RDKY2926 was cotransformed with the indicated combination of one bait plasmid and one prey plasmid, and the transformants were replica plated onto Ura⁻His⁻Trp⁻ 5-bromo-4-chloro-3-indolyl β -D-galactoside (X-Gal) glucose and Ura⁻His⁻Trp⁻ X-Gal galactose indicator plates and incubated at 30°C for 2 days.

only functions in the repair of insertion/deletion mismatches (1, 15, 40) and is most uniquely important for the repair of insertion/deletion mismatches larger than two unpaired bases (37). These two complexes are most redundant for the recognition of single-base insertion/deletion mismatches (1, 15, 37). Similarly, a heterodimer of two MutL-related proteins, MLH1 and PMS1 (PMS2 in humans), functions as the MutL equivalent (1, 2, 19, 21).

The studies presented here suggest there is a second heterodimeric complex of MutL-related proteins, MLH1 and MLH3, that can partially substitute for the MLH1–PMS1 complex in the repair of mismatched bases recognized by the MSH2–MSH3 complex (Fig. 5). A number of lines of evidence support this view. First, full-length MLH3 interacts with MLH1. This finding is consistent with previous studies demonstrating that MLH3 contains amino acid sequences that are conserved in the yeast PMS1 and human PMS2 proteins in a region that is crucial for the interaction of these proteins with MLH1 (23). Second, mutations in *MLH3* cause a small but significant increase in the rate of accumulation of single-base frameshift mutations similar to that caused by mutations in *MSH3*; epistasis analysis consistent with the idea that these two genes are in the same pathway. Third, mutations in *MLH3*

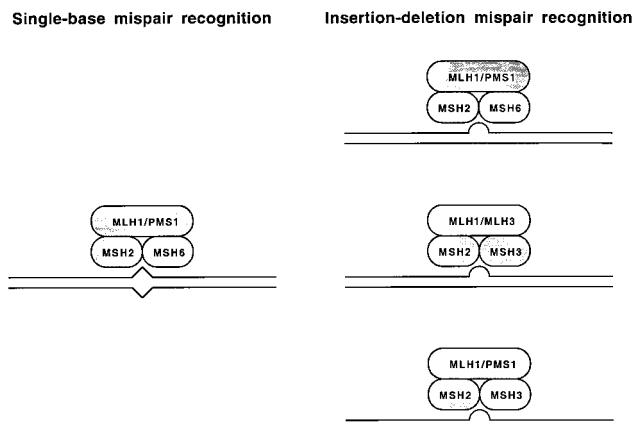


FIG. 5. Model of action of MLH3 in mismatch repair. Note that specific contacts between individual MLH and MSH proteins are not meant to be implied by this model as no information is presently available about such contacts.

significantly increase the rate of accumulation of frameshifts in strains lacking *MSH6* consistent with the view that mutations in *MLH3* cause defects in MSH3-dependent repair. And fourth, the *mlh3 pms1* double mutant consistently had a greater mutation rate in the *hom3-10* reversion assay than either single mutant, suggesting that at least for some mutation events, inactivation of both *MLH3* and *PMS1* is required to produce the greatest inactivation of mismatch repair.

There are several features of our data that should be commented on further. First, the *mlh3 msh6* double mutant has at most 15% the mutation rate of a *msh2* mutant or a *msh3 msh6* double mutant. This finding indicates that only a portion of MSH3-dependent repair requires the MLH1-MLH3 complex. It is unlikely that any MLH3-independent repair involves the other MutL homolog MLH2 because mutations in *MLH2* do not cause a mutator phenotype nor do they increase the mutator phenotype caused by mutations in *MLH3* (A. Datta, H.F.-R. and R.D.K., unpublished results). Thus, the remainder of the repair most likely involves the MLH1-PMS1 complex. Second, in our analysis of the effects of *msh3*, *msh6*, and *mlh3* single mutations and the *mlh3 msh6* double mutation combination on the accumulation of frameshift mutations at specific frameshift hot spots, we have observed considerable hot spot to hot spot variation (compare the *lys2-Bgl* spectra presented in Fig. 3). The differences in mutation spectra and hot spot-specific mutation rates seen in *msh3* and *msh6* mutants in this and other studies most likely reflect differences in the specificity of the MSH2-MSH3 and MSH2-MSH6 complexes for different insertion/deletion mispairs (15, 39). In the case of the *mlh3 msh6* double mutation combination, the increase in mutation rate compared with wild type ranged from 4.5- to 86-fold. This suggests that the ability of the MLH1-MLH3 complex to productively interact with a MSH2-MSH3-mismatch complex depends on the mispair. Exactly what features of the MSH complex-mismatch complex that allows productive interactions with other mismatch repair proteins and how these features vary depending on the mispair are unknown at present. An important implication of these results is that to study the biochemical role of the MLH1-MLH3 and MSH2-MSH3 complexes in mismatch repair, it will be important to identify mispair containing substrates whose repair is dependent on these complexes. It also should be pointed out that the source of the mispair, replication errors in our study, but possibly recombination or DNA-damaging agents in other circumstances, could affect which MSH and MLH complexes are targeted to the mispair to promote repair.

It is interesting to note that when compared with other known MutL homologs, MLH3 is most related to the PMS proteins (Fig. 1) and in particular to human PMS1. The homology between MLH3 and hPMS1 extends throughout the entire predicted amino acid sequences of these two proteins. The greatest region of identity is between residues 1-120 of MLH3 and hPMS1. Importantly, MLH3, hPMS1, and hPMS2 show high conservation of sequences present in the C-terminal region of yeast PMS1, a region which is thought to be crucial for interaction with MLH1 (23). A role for hPMS1 in mismatch repair has been suggested by the finding of a germ-line mutation in this gene in one patient with colon cancer (22). It is tempting to speculate that hPMS1 may carry out a similar role in human mismatch repair as MLH3 does in yeast. If this were the case, mutations in *hPMS1* would be expected to cause only a weak mutator phenotype, possibly explaining why so few cases of cancer involving *hPMS1* have been reported. This view has been substantiated in experiments with mice containing mutations in *PMS1* (41). Furthermore, because hPMS1 would be expected to be partially redundant with hPMS2, this would help explain the reduced number of hereditary non-

polyposis colorectal carcinoma causing germ-line mutations reported in *hPMS2* compared with the large number reported in *hMLH1* (1, 9).

We thank Neelam Amin, Clark Chen, Ruchira Das Gupta, Abhijit Datta, Alex Shoemaker, and Dan Tishkoff for comments on the manuscript and John Weger and Jill Green for DNA sequencing. H. F.-R. is a fellow of The Jane-Coffin Childs Memorial Fund for Medical Research. This work also was supported by National Institutes of Health Grant GM50006 (to R.D.K.).

- Kolodner, R. (1996) *Genes Dev.* **10**, 1433-1442.
- Modrich, P. & Lahue, R. (1996) *Annu. Rev. Biochem.* **65**, 101-133.
- Ceccotti, S., Aquilina, G., Macpherson, P., Yamada, M., Karran, P. & Bignami, M. (1996) *Curr. Biol.* **6**, 1528-1531.
- Fram, R. J., Cusick, P. S., Wilson, J. M. & Marinus, G. M. (1985) *Mol. Pharmacol.* **28**, 51-55.
- Karran, P. & Marinus, M. G. (1982) *Nature (London)* **296**, 868-869.
- Selva, E. M., Maderazo, A. B. & Lahue, R. S. (1997) *Mol. Gen. Genet.* **257**, 71-82.
- Rayssiguier, C., Thaler, D. S. & Radman, M. (1989) *Nature (London)* **342**, 396-401.
- Datta, A., Hendrix, M., Lipsitch, M. & Jinks-Robertson, S. (1997) *Proc. Natl. Acad. Sci. USA* **94**, 9757-9762.
- Peltomaki, P. & Vasen, H. F. (1997) *Gastroenterology* **113**, 1146-1158.
- Dietmaier, W., Wallinger, S., Bocker, T., Kullmann, F., Fishel, R. & Ruschoff, J. (1997) *Cancer Res.* **57**, 4749-4756.
- Kane, M. F., Loda, M., Gaida, G. M., Lipman, J., Mishra, R., Goldman, H., Jessup, J. M. & Kolodner, R. (1997) *Cancer Res.* **57**, 808-811.
- Thibodeau, S. N., French, A. J., Cunningham, J. M., Tester, D., Burgart, L. J., Roche, P. C., McDonnell, S. K., Schaid, D. J., Vockley, C. W., Michels, V. V., et al. (1998) *Cancer Res.* **58**, 1713-1718.
- Viswanathan, M. & Lovett, S. T. (1998) *Genetics* **149**, 7-16.
- Crouse, G. F. (1998) in *DNA Repair in Prokaryotes and Lower Eukaryotes*, eds. Nickoloff, J. A. & Hoekstra, M. F. (Humana, Totowa, NJ), Vol. 1, pp. 411-448.
- Marsischky, G. T., Filosi, N., Kane, M. F. & Kolodner, R. (1996) *Genes Dev.* **10**, 407-420.
- Drummond, J. T., Li, G. M., Longley, M. J. & Modrich, P. (1995) *Science* **268**, 1909-1912.
- Acharya, S., Wilson, T., Gradia, S., Kane, M. F., Guerrette, S., Marsischky, G. T., Kolodner, R. & Fishel, R. (1996) *Proc. Natl. Acad. Sci. USA* **93**, 13629-13634.
- Palombo, F., Gallinari, P., Iaccarino, I., Lettieri, T., D'arrigo, A., Truong, J., Hsuan, J. & Jiricny, J. (1995) *Science* **268**, 1912-1914.
- Prolla, T. A., Pang, Q., Alani, E., Kolodner, R. D. & Liskay, R. M. (1994) *Science* **265**, 1091-1093.
- Prolla, T. A., Christie, D. M. & Liskay, R. M. (1994) *Mol. Cell. Biol.* **14**, 407-415.
- Li, G.-M. & Modrich, P. (1995) *Proc. Natl. Acad. Sci. USA* **92**, 1950-1954.
- Nicolaides, N. C., Papadopoulos, N., Liu, B., Wei, Y., Carter, K. C., Ruben, S. M., Rosen, C. A., Haseltine, W. A., Fleischmann, R. D., Fraser, C. M., et al. (1994) *Nature (London)* **371**, 75-80.
- Pang, Q., Prolla, T. A. & Liskay, R. M. (1997) *Mol. Cell. Biol.* **17**, 4465-4473.
- Alani, E., Reenan, R. A. G. & Kolodner, R. (1994) *Genetics* **137**, 19-39.
- Tishkoff, D. X., Filosi, N., Gaida, G. M. & Kolodner, R. D. (1997) *Cell* **88**, 253-263.
- Manivasakam, P., Weber, S. C., McElver, J. & Schiestl, R. H. (1995) *Nucleic Acids Res.* **23**, 2799-2800.
- Rothstein, R. (1991) *Methods Enzymol.* **194**, 281-301.
- Christianson, T. W., Sikorski, R. S., Dante, M., Shero, J. H. & Hieter, P. (1992) *Gene* **110**, 119-122.
- Lea, D. E. & Coulson, C. A. (1948) *J. Genet.* **49**, 264-268.
- Hoffman, C. S. & Winston, F. (1987) *Gene* **57**, 267-272.
- Gyuris, J., Golemis, E., Chertkov, H. & Brent, R. (1993) *Cell* **75**, 791-803.
- Jeyaprakash, A., Das Gupta, R. & Kolodner, R. (1996) *Mol. Cell. Biol.* **16**, 3008-3011.
- Golemis, E. A. & Brent, R. (1992) *Mol. Cell. Biol.* **12**, 3006-3014.
- Estojak, J., Brent, R. & Golemis, E. A. (1995) *Mol. Cell. Biol.* **15**, 5820-5829.
- Finley, R. L. & Brent, R. (1994) *Proc. Natl. Acad. Sci. USA* **91**, 12980-12984.
- New, L., Liu, K. & Crouse, G. F. (1993) *Mol. Gen. Genet.* **239**, 97-108.
- Sia, E. A., Kokoska, R. J., Dominska, M., Greenwell, P. & Petes, T. D. (1997) *Mol. Cell. Biol.* **17**, 2851-2858.
- Mo, J. Y., Maki, H. & Sekiguchi, M. (1991) *J. Mol. Biol.* **222**, 925-936.
- Greene, C. N. & Jinks-Robertson, S. (1997) *Mol. Cell. Biol.* **17**, 2844-2850.
- Strand, M., Earley, M. C., Crouse, G. F. & Petes, T. D. (1995) *Proc. Natl. Acad. Sci. USA* **92**, 10418-10421.
- Prolla, T. A., Baker, S. M., Harris, A. C., Tsao, J. L., Yao, X., Bronner, C. E., Zheng, B., Gordon, M., Reneker, J., Arnheim, N., et al. (1998) *Nat. Genet.* **18**, 276-279.